Available at
www.ElsevierComputerScience.com
POWERED BY SCIENCE DIRECT
Computer Aided Geometric Design 20 (2003) 621–636
COMPUTER AIDED GEOMETRIC DESIGN
www.elsevier.com/locate/cagd

The shape of spherical quartics

Bert Jüttler [a,*], Wenping Wang [b]

[a] *Johannes Kepler University, Institute of Analysis, Department of Applied Geometry, Altenberger Str. 69, 4040 Linz, Austria*
[b] *The University of Hong Kong, Department of Computer Science and Information Systems, Pokfulam Road, Hong Kong, China*

Received 27 May 2003; accepted 7 July 2003

Dedicated to the memory of Professor Dr. Josef Hoschek

Abstract

We discuss the problem of interpolating C^1 Hermite data on the sphere (two points with associated first derivative vectors) by spherical rational curves. With the help of the generalized stereographic projection (Dietz et al., 1993), we construct a two-parameter family of spherical quartics solving this problem. We study the shape of these solutions and derive criteria which guarantee solutions without cusps or self-intersections.

Keywords: Hermite interpolation; Spherical rational curves; Generalized stereographic projection

1. Introduction

Spherical curves, and rational spherical curves in particular, have various applications. These include techniques for motion design in robot kinematics and computer animation (Jüttler and Wagner, 2002; Röschel, 1998), and algorithms for the construction of Pythagorean hodograph curves (Farouki et al., 2002; Farouki, 2002). Several methods for generating spherical curves are available. Spherical generalizations of de Casteljau's algorithm, which are used in Computer Graphics (e.g., (Pletinckx, 1989; Shoemake, 1985), lead to non-rational spline curves with rather complicated coordinate functions. This entails nonlinear interpolation conditions, difficulties with the construction of C^2 curves and the lack of a subdivision property (Nielson and Heiland, 1992). Other approaches are based on mappings into the plane (Jupp and Kent, 1987) arc splines (Hoschek and Seemann, 1992), biarcs (Wang and Joe, 1993, 1997), blending methods (Kim and Nam, 1995), spherical generalizations of the cumulative form of

* Corresponding author.
E-mail addresses: bert.juettler@jku.at (B. Jüttler), wenping@csis.hku.hk (W. Wang).

0167-8396/$ – see front matter © 2003 Published by Elsevier B.V.
doi:10.1016/j.cagd.2003.07.003

B-spline-curves (Kim et al., 1995), spherical Lagrange interpolation (Gfrerrer, 1999) and generalized corner cutting (Noakes, 1998).

Rational curves on quadric surfaces (e.g., on the sphere) can be seen as solutions to certain Diophantine equations in the ring of polynomials. In the three-dimensional case, the equation of the unit sphere $\mathbb{S}^2$ (which is a representative of the class of oval quadrics) takes the form $w^2 = x^2 + y^2 + z^2$. All irreducible solutions can be generated with the help of a classical representation formula from number theory, which was first noted by V.A. Lebesgue in 1868 (Dickson, 1952).

This formula has been used to define a mapping from real projective 3-space onto the unit sphere, $\delta : P^3(\mathbb{R}) \to \mathbb{S}^2$, which has been called the *generalized stereographic projection* (Dietz et al., 1993), since it comprises the standard stereographic projection as a special case. As a major advantage, this mapping avoids the dependency on the choice of the center of projection, which is always present for the standard stereographic projection. Due to its algebraic origin, this mapping can be used to generate any rational curve of degree $2n$ on the sphere as the image of a curve of degree n.

This mapping can be discussed from a geometrical point of view, too. It can be shown to identify the points of the unit sphere with a special two-parameter system of lines, called an elliptic linear congruence. See the textbook by Pottmann and Wallner (2001), where the generalized stereographic projection appears as the famous "Hopf mapping", for more information on this point of view. Also, the mapping is closely related to quaternion calculus and the Eulerian representation of special orthogonal matrices (Jüttler and Wagner, 2002). Another possible framework, based on Clifford algebras, is described by Choi et al. (2002).

We use the generalized stereographic projection to generate and to analyze the solutions to the C^1 Hermite interpolation problem with spherical rational curves on the sphere $\mathbb{S}^2$ in three-dimensional space. Given two points with associated first derivatives on a sphere, we interpolate this data with a spherical rational quartic.

Recently, rational quartics on the hypersphere $\mathbb{S}^3$ in four-dimensional space have been used by Wang and Qin (2000) for solving the C^1 Hermite interpolation problem. The data (two points with associated first derivative vector) spans a hyperplane, and it is natural to study those solutions which are contained in this hyperplane, i.e., three-dimensional solutions (although other solutions exist too). In this paper we restrict ourselves to these solutions, leading to a two-parameter family of solutions.

Using the generalized stereographic projection, each solution can be identified with a point in a certain parameter plane. We discuss the shape of the solutions, which is characterized by the presence of cusps or double points. This results in a so-called *characterization diagram*: the parameter plane is subdivided in different regions which correspond to solutions with the same shape.

2. Preliminaries

Throughout this paper we use *homogeneous coordinates* $\mathbf{p} = (p_0, p_1, p_2, p_3) \neq (0, 0, 0, 0)$ to describe points in 3-space. If two vectors $\mathbf{p}$, $\mathbf{p}'$ of homogeneous coordinates are linearly dependent, i.e., $\mathbf{p} = \rho\,\mathbf{p}'$ for some $\rho \neq 0$, then they correspond to the same point in 3-space.

If $p_0 \neq 0$ holds, then the associated *Cartesian coordinates* of the point $\mathbf{p}$ are $\mathbf{P} = (p_1/p_0, p_2/p_0, p_3/p_0)$. Otherwise, if $p_0 = 0$, the coordinates $\mathbf{p}$ correspond to a so-called *ideal point*; it can be used to represent the intersection point of all lines with a direction parallel to the vector (p_1, p_2, p_3). Capital respectively lowercase letters are used to denote Cartesian respectively homogeneous coordinates.

With the help of homogeneous coordinates, the equation of the unit sphere in 3-space can be rewritten as

$$x_0^2 = x_1^2 + x_2^2 + x_3^2. \tag{1}$$

Any quadruple of polynomials $x_0(t), \ldots, x_3(t)$ which satisfies this equation defines a spherical rational curve $\mathbf{x}(t) = (x_0(t), \ldots, x_3(t))$.

In order to generate rational curves and surfaces on the unit sphere, the *generalized stereographic projection* has been introduced by Dietz et al. (1993). For the convenience of the reader, we summarize the main properties.

The generalized stereographic projection maps a point $\mathbf{p}$ in three-dimensional space to the point

$$\delta(\mathbf{p}) = \bigl(p_0^2+p_1^2+p_2^2+p_3^2,\ 2p_0p_1-2p_2p_3,\ 2p_1p_3+2p_0p_2,\ p_1^2+p_2^2-p_0^2-p_3^2\bigr) \tag{2}$$

on the unit sphere. Indeed, the point $\mathbf{x} = \delta(\mathbf{p})$ satisfies (1).

By restricting the generalized stereographic projection to the xy-plane, (i.e., by choosing points with $p_3 = 0$), one gets the standard stereographic projection, with the center at the north pole $\mathbf{n} = (1, 0, 0, 1)$ of the sphere.

This mapping is based on a representation formula for irreducible Pythagorean quadruples in number theory which is attributed to V.A. Lebesgue (Dickson, 1952). Due to its algebraic properties, any rational spherical curve of degree $2n$ can be constructed by applying δ to a rational space curve of degree n.

For instance, any spherical curve of degree two, i.e., any *circle*, can be obtained as the image of a *line* in $P^3(\mathbb{R})$. Applying the standard stereographic projection to lines in the xy-plane, by contrast, gives only those circles which pass through the center of projection. Similarly, any spherical rational *quartic* can be generated by applying the generalized stereographic projection to a rational curve of degree 2, i.e., to a *conic*. This observation will be exploited in this paper.

The generalized stereographic projection is not a one-to-one mapping, as points in 3-space are mapped to a surface. Any *point* on the sphere corresponds to a *line* in 3-space. Any of these lines is called a *projecting line*.

In contrast to the more familiar case of a perspective projection, the projecting lines do not pass through a single center, but form a more sophisticated system of lines instead. For any point $\mathbf{p} = (p_0, p_1, p_2, p_3)$, let $\mathbf{p}^\perp = (-p_3, p_2, -p_1, p_0)$. The line spanned by $\mathbf{p}$ and $\mathbf{p}^\top$ is then a projecting line; all its points are mapped to the same point on the unit sphere. A short calculation indeed confirms that, for arbitrary coefficients λ, μ,

$$\delta(\lambda\mathbf{p} + \mu\mathbf{p}^\perp) = \bigl(\lambda^2 + \mu^2\bigr)\delta(\mathbf{p}). \tag{3}$$

Since we are using homogeneous coordinates, all points on the line spanned by $\mathbf{p}$ and $\mathbf{p}^\top$ are mapped to the same point.

The system of all lines of the form $\lambda\mathbf{p} + \mu\mathbf{p}^\perp$ has a space-filling property: *any point in three-space lies on exactly one line*. These lines can be shown to form a so-called linear congruence: they all pass through two fixed *focal lines*, which are, however, conjugate-complex in our situation. For all points on the two focal lines, the four components of (2) vanish simultaneously. Consequently, the focal lines consist of all base points of the generalized stereographic projection. See Dietz et al. (1993) or Pottmann and Wallner (2001) for more details.

3. Hermite interpolation with spherical quartics

We study the problem of C^1 Hermite interpolation with spherical rational curves. Given two points $\mathbf{Q}_0$ and $\mathbf{Q}_1$ on the sphere with associated first derivatives (tangent vectors) $\vec{\mathbf{D}}_0$ and $\vec{\mathbf{D}}_1$, we want to find a spherical rational curve $\mathbf{X}(t)$ with domain $t \in [0, 1]$ such that

$$\mathbf{X}(0) = \mathbf{Q}_0, \quad \frac{\mathrm{d}}{\mathrm{d}t}\mathbf{X}(t)\bigg|_{t=0} = \vec{\mathbf{D}}_0, \quad \mathbf{X}(1) = \mathbf{Q}_1, \quad \text{and} \quad \frac{\mathrm{d}}{\mathrm{d}t}\mathbf{X}(t)\bigg|_{t=1} = \vec{\mathbf{D}}_1. \tag{4}$$

This problem can be solved by rational curves of degree 4, the so-called rational *spherical quartics*. In homogeneous coordinates $\mathbf{x} = (x_0, x_1, x_2, x_3)$, these curves are described by four quartic polynomials $x_i = x_i(t)$. This corresponds to rational Cartesian coordinate functions $\mathbf{X} = (x_1/x_0, x_2/x_0, x_3/x_0)$.

Note that the given data includes not only the tangents, but also the *length* of the boundary derivatives, i.e., the parametric speed at $t = 0$ and $t = 1$! Consequently, the solution to this problem can easily be used to construct C^1 spline curves. The parametric speed may be important for applications in computer animation or kinematics, where spherical curves correspond to rotations. Here, the interpolation of a given (angular) velocity distribution can sometimes be desirable.

In order to simplify the analysis of the solutions, we assume that the C^1 boundary data is given in a certain standard form, as follows. First, the points $\mathbf{Q}_0$ and $\mathbf{Q}_1$ are assumed to be in the lower half of the xz-plane. Second, their bisector in the xz-plane is assumed to be the z-axis. Then, using the well-known parameterization of a circle by $q = \tan\frac{\phi}{2}$, the boundary points can easily be represented as

$$\mathbf{Q}_0 = \left(\frac{-2q}{q^2+1}, 0, \frac{q^2-1}{q^2+1}\right), \quad \text{and} \quad \mathbf{Q}_1 = \left(\frac{2q}{q^2+1}, 0, \frac{q^2-1}{q^2+1}\right) \tag{5}$$

with a constant $q \in [0, 1]$. The given tangent vectors $\vec{\mathbf{D}}_0$ at $\mathbf{Q}_0$ and $\vec{\mathbf{D}}_1$ at $\mathbf{Q}_1$ can be represented as

$$\vec{\mathbf{D}}_0 = \frac{1}{q^2+1}\big(T_1(q^2-1), T_2, 2T_1 q\big) \tag{6}$$

and

$$\vec{\mathbf{D}}_1 = \frac{1}{q^2+1}\big(S_1(q^2-1), S_2, -2S_1 q\big), \tag{7}$$

where T_1, T_2, and S_1, S_2 are certain constants.

We assume that neither of the given tangent vectors vanishes and that the two endpoints are different. Hence, $(T_1, T_2) \neq (0, 0)$, $(S_1, S_2) \neq (0, 0)$, and $q \neq 0$.

We call the given data *circular*, if it can be matched by a circular arc.[1] This the case if and only if the two points $\mathbf{Q}_0$, $\mathbf{Q}_1$ and the tangent vectors $\vec{\mathbf{D}}_0$, $\vec{\mathbf{D}}_1$ are coplanar.

4. Canonical form of the solutions

We give an explicit representation of the family of solutions, depending on two free parameters X and Y. The solutions matching a given set of C^1 Hermite boundary data have two degrees of freedom; consequently, they can be identified with a point in the XY-plane.

[1] Here we consider general quartic representations of the circular arc.

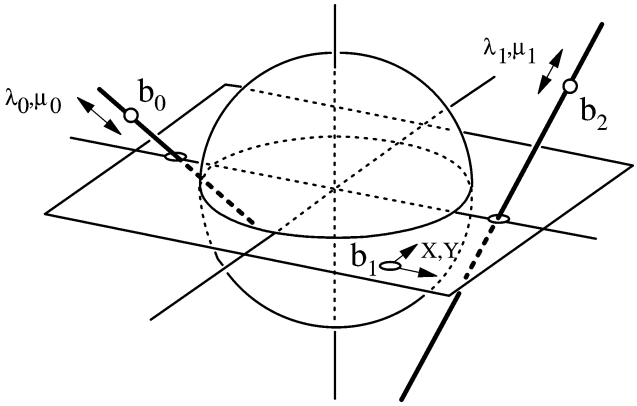

Fig. 1. Choosing the preimage control points of the spherical quartic.

4.1. Preimage curve

In order to construct an interpolating spherical quartic curve, we apply the generalized stereographic projection to a quadratic rational preimage curve, i.e., to an arc of a conic section (conic for short). The preimage curve is given as a rational curve of degree 2 in Bézier form, with the parameterization

$$\mathbf{p}(t) = (1-t)^2\mathbf{b}_0 + 2t(1-t)\mathbf{b}_1 + t^2\mathbf{b}_2, \quad t \in [0,1]. \tag{8}$$

Due to the properties of the generalized stereographic projection, any curve of the pencil $\lambda\mathbf{p}(t) + \mu\mathbf{p}(t)^\perp$ ($\lambda, \mu \in \mathbb{R}$) is mapped to the same quartic curve. Thus, we may—without loss of generality—pick one of these preimages. We do so by constraining the weight and the location of the inner control point; its weight is normalized to be 1, and its location is constrained to the xy-plane,[2]

$$\mathbf{b}_1 = (1, X, Y, 0). \tag{9}$$

The two boundary control points of the preimage curve are chosen as

$$\begin{aligned} \mathbf{b}_0 &= \lambda_0\,(1, -q, 0, 0) + \mu_0\,(0, 0, q, 1), \quad \text{and} \\ \mathbf{b}_2 &= \lambda_1\,(1, q, 0, 0) + \mu_1\,(0, 0, -q, 1). \end{aligned} \tag{10}$$

These are arbitrary points on the preimage lines of the two given boundary points $\mathbf{Q}_0$ and $\mathbf{Q}_1$, with arbitrary weights. Consequently, the image curve $\delta(\mathbf{p})$ matches these points. The position and the weights of the control points depend on the six parameters X, Y, λ_0, λ_1, μ_0 and μ_1.

4.2. Image curve

We apply the generalized stereographic projection (2) to the quadratic curve (8). This results in the quartic Bézier curve $\mathbf{x}(t) = \delta(\mathbf{p}(t))$,

$$\mathbf{x}(t) = (1-t)^4\mathbf{c}_0 + 4(1-t)^3t\mathbf{c}_1 + 6(1-t)^2t^2\mathbf{c}_2 + 4(1-t)t^3\mathbf{c}_3 + t^3\mathbf{c}_4, \tag{11}$$

[2] The pencil of curves has two degrees of freedom, which are used to satisfy the two constraints. The weight normalization excludes inner control points at infinity. This special case can be studied by considering the limit $(X, Y) = (\gamma X_0, \gamma Y_0)$, where $\gamma \to \infty$.

with the control points

$$\mathbf{c}_0 = (\lambda_0^2 + \mu_0^2)\ \underbrace{(q^2+1,\ -2q,\ 0,\ q^2-1)}_{=\mathbf{q}_0}, \tag{12}$$

$$\mathbf{c}_1 = (-\lambda_0 qX + \mu_0 qY + \lambda_0,\ \lambda_0 X - \mu_0 Y - \lambda_0 q, \mu_0 X + \lambda_0 Y + \mu_0 q,\ -\lambda_0 qX + \mu_0 qY - \lambda_0), \tag{13}$$

$$\mathbf{c}_2 = \frac{1}{3}\big(2X^2 + 2Y^2 + (\lambda_0\lambda_1 + \mu_0\mu_1)(1-q^2) + 2, 4X, 4Y + 2\mu_0\lambda_1 q - 2\lambda_0\mu_1 q, 2X^2 + 2Y^2 - (\lambda_0\lambda_1 + \mu_0\mu_1)(1+q^2) - 2\big), \tag{14}$$

$$\mathbf{c}_3 = (\lambda_1 qX - \mu_1 qY + \lambda_1, \lambda_1 X - \mu_1 Y + \lambda_1 q, \mu_1 X + \lambda_1 Y - \mu_1 q, \lambda_1 qX - \mu_1 qY - \lambda_1) \tag{15}$$

and

$$\mathbf{c}_4 = (\lambda_1^2 + \mu_1^2)\ \underbrace{(q^2+1,\ 2q,\ 0,\ q^2-1)}_{=\mathbf{q}_1}. \tag{16}$$

As we chose the boundary control points $\mathbf{b}_0$, $\mathbf{b}_2$ of the preimage curve on the projecting lines (10), the boundary control points $\mathbf{c}_0$, $\mathbf{c}_4$ of the quartic curve match the given points $\mathbf{Q}_0$, $\mathbf{Q}_1$.

In the next step, we may choose the parameters λ_0, λ_1, μ_0, and μ_1 in order to match the given derivative data, cf. (6) and (7). After some (computer) algebra one arrives at

$$\lambda_0 = 4\,\frac{T_2 Y - T_1(q^2+1)(X+q)}{T_1^2(q^2+1)^2 + T_2^2}, \qquad \mu_0 = 4\,\frac{T_2(X+q) + T_1 Y(q^2+1)}{T_1^2(q^2+1)^2 + T_2^2} \tag{17}$$

and

$$\lambda_1 = 4\,\frac{S_1(q^2+1)(X-q) - S_2 Y}{S_1^2(q^2+1)^2 + S_2^2}, \qquad \mu_1 = 4\,\frac{S_2(q-X) - S_1 Y(q^2+1)}{S_1^2(q^2+1)^2 + S_2^2}. \tag{18}$$

The numerators of these expressions vanish if and only if the Hermite data is singular, i.e., $\vec{\mathbf{D}}_0 = \vec{\mathbf{0}}$ or $\vec{\mathbf{D}}_1 = \vec{\mathbf{0}}$. Summarizing, we have the following result.

Theorem 1. *The spherical rational quartic curves which match the C^1 Hermite boundary data* (4) *have the form* (11) *with the control points* (12)–(16) *and the parameters λ_i and μ_i as in* (17), (18).

Thus, after taking the Hermite data into account, we obtain a two-parameter family of solutions. The two free parameters are the two coordinates (X, Y) of the inner control point $\mathbf{b}_1$ of the preimage curve. If the data is non-circular, then different parameters (X, Y) also produce different solutions. It can be shown that any two quadratic preimages of a spherical quartic belong to the same pencil $\lambda\mathbf{p}(t) + \mu\mathbf{p}(t)^\perp$ of quadratic curves, and each such pencil contains only one curve with an inner control point of the form $(1, X, Y, 0)$. Consequently, we have (for non-circular data) a one-to-one correspondence between the solutions of the Hermite interpolation problem and the points $(X, Y) \in \mathbb{R}^2$.

5. Shape analysis

Based on the previous theorem, we analyze the shape of the interpolating curves. In particular, we will characterize solutions with double points and cusps.

5.1. Global classification

We begin our analysis by considering the spherical quartic curve (11) with the *extended* parameter domain $t \in \mathbb{R} \cup \{\infty\}$. Its shape can be classified as follows.

- *Case* 1 (*degenerate*). The preimage curve (8) is contained in a projecting line (3). Consequently, the spherical quartic curve degenerates into a *single point*. This curve matches the degenerate Hermite data $\mathbf{Q}_0 = \mathbf{Q}_1$ and $\vec{\mathbf{D}}_0 = \vec{\mathbf{D}}_1 = \vec{\mathbf{0}}$, i.e., $q = T_1 = T_2 = S_1 = S_2 = 0$.
- *Case* 2 (*singular*). The preimage curve (8) is contained in a line, which is not a projecting line. Consequently, the spherical quartic curve degenerates into a *circle* (if the preimage curve traces the entire line) or into a circular arc (if the preimage curve traces a line segment only, which is then covered twice). This case may occur only if the given Hermite boundary data is coplanar, as they cannot be matched by a single circular arc otherwise.
- *Case* 3 (*general*). The preimage curve (8) is a non-degenerate conic. Clearly, the control points $\mathbf{b}_0$, $\mathbf{b}_1$ and $\mathbf{b}_2$ span a plane π, and the conic is contained in this plane. Due to the properties of the generalized stereographic projection (see (Dietz et al., 1993)), the plane π contains exactly one projecting line[3] ℓ_π. Depending on the relative position of this line with respect to the preimage conic, we arrive at three different sub-cases.
  - *Case* 3.1 (*hyperbolic*). The line ℓ_π intersects the conic in two real and distinct points. Consequently, the spherical quartic curve has a single double point with two real parameter values.
  - *Case* 3.2 (*elliptic*). The line ℓ_π intersects the conic in two conjugate-complex and distinct points.
    - *Case* 3.2.1 (*regular*). The two intersections do not belong to the two focal lines. The spherical quartic curve does not have a double point. More precisely, the curve has an isolated double point, but with two conjugate-complex parameter values.
    - *Case* 3.2.2 (*singular*). The two intersections belong to the two focal lines. Consequently, the spherical quartic curve degenerates into a circle, since the components of $\delta(\mathbf{p}(t))$ share a quadratic factor. Its roots are the conjugate-complex parameter values of the intersections with ℓ_π.

      Similar to Case 2, this case may occur only if the given Hermite boundary data is coplanar, as they cannot be matched by a single circular arc otherwise.
  - *Case* 3.3 (*parabolic*). The line ℓ_π is tangent to the conic. The tangent point is necessarily real, thus not on either of the two focal lines. We obtain a spherical quartic curve with a cusp.

Some examples for Case 3 are shown in Fig. 2.

Clearly, as we want to analyze the solutions to the Hermite interpolation problem (4), we are mostly interested in the properties of the curve *segment* $t \in [0, 1]$. This segment may have a double point or a cusp. Among the two-parameter family of solutions (see Theorem 1), there are three transition cases between the different types of solutions. These are the curves with a *cusp*, and curves with *double points* at the boundaries (at $t = 0$ or at $t = 1$).

[3] Recall that the projecting lines pass through two conjugate-complex focal lines. The line ℓ_π is spanned by the two intersections of the plane π with the focal lines.

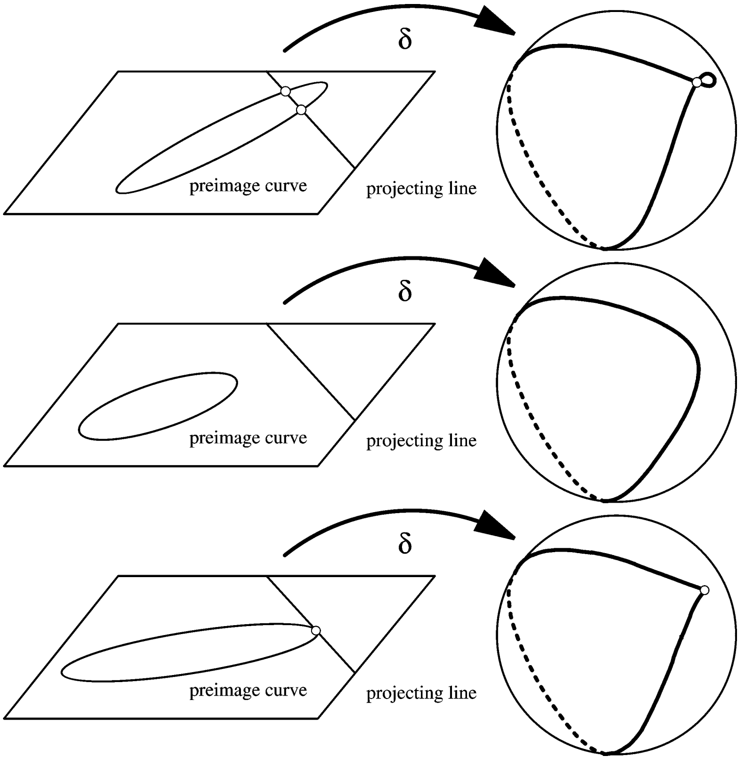

Fig. 2. Hyperbolic, elliptic (regular) and parabolic case.

5.2. Cusps

Assume that the quartic curve is not a circular arc. The image of the quadratic rational Bézier curve $\mathbf{p}(t)$ (see (8)) under the generalized stereographic projection δ has a cusp for some $t = t_0$ if the tangent at $\mathbf{p}(t_0)$ is a projecting line.

Recall that the tangent of a curve $\mathbf{p}(t)$ is spanned by the point $\mathbf{p}(t)$ and by the associated *derivative point* $\dot{\mathbf{p}}(t)$. Let

$$g_{ij}(t) = p_i(t)\dot{p}_j(t) - p_j(t)\dot{p}_i(t), \quad i, j = 0, \ldots, 3, \tag{19}$$

be the *Plücker coordinates*[4] of the tangent. As observed by Dietz et al. (1993), the projecting lines of the generalized stereographic projection are uniquely characterized by the two linear equations $g_{01} - g_{23} = 0$ and $g_{02} - g_{31} = 0$ of the Plücker coordinates. Consequently, if the two polynomials

$$G(t) = g_{01}(t) - g_{23}(t) \quad \text{and} \quad H(t) = g_{02}(t) - g_{31}(t) \tag{20}$$

have the simultaneous root $t = t_0$, then either the tangent of the preimage curve at $\mathbf{p}(t_0)$ is a projecting line, or the preimage curve is singular at $t = t_0$, i.e., $\mathbf{p}(t_0)$ and the derivative point $\mathbf{p}(t_0)$ are linearly

[4] Taking the antisymmetry into account, the g_{ij} form a system of 6 homogeneous coordinates which uniquely characterize the lines in three-dimensional space. A more detailed introduction to line geometry is beyond the scope of the present paper. The interested reader should consult the textbook of Pottmann and Wallner (2001).

dependent. The second case was excluded by assuming a non-circular spherical quartic. The first case corresponds to a cusp of the spherical quartic curve $\mathbf{x}(t)$.

Both $G(t)$ and $H(t)$ are polynomials of degree 2 in t and of degree 2 in X, Y. Using computer algebra tools we compute the resultant of $G(t)$ and $H(t)$ with respect to the parameter t,

$$c(X,Y) = \frac{(T_1^2(q^2+1)^2+T_2^2)^2(S_1^2(q^2+1)^2+S_2^2)^2}{4096}\operatorname{Res}\big(G(t), H(t), \{t\}\big). \tag{21}$$

The Maple code of these computations is given in Appendix A. The resultant is a polynomial of degree 8 in X, Y.

The resultant vanishes if any only if both polynomials have a common root $t = t_0$. Consequently, the quartic curve $\mathbf{x}(t)$ has a cusp for some $t = t_0$ if and only if the resultant vanishes. The set of all points in the XY-plane with $c(X,Y) = 0$ forms an algebraic curve $\mathcal{C}$ in the plane; this curve will be referred to as the *cusp curve*. The cusp curve is symmetric with respect to the Y-axis. It intersects the X-axis in the points $(\pm q, 0)$, where each of these points has multiplicity 4.

Proposition 2. *Assume that the Hermite data is non-circular. The cusp curve $\mathcal{C}$ factors into four circles. All these circles pass through the two points $(\pm q, 0)$, and they are symmetric with respect to the Y-axis.*

Proof. The two points $(\pm q, 0)$ and the circular points at infinity (with homogeneous coordinates $(0, 1, \pm i)$, where i is the imaginary unit) are 4-fold points of the cusp curve. This can be shown by substituting these points into the equation of the cusp curve and its derivatives. Furthermore, it is straightforward to verify that none of the six lines determined by the four 4-fold points is a component of the cusp curve, provided that the data is non-circular.

Now we claim that, other than the four 4-fold points, any point $\mathbf{r}$ of the cusp curve is not on any of the six lines determined by the four 4-fold points. For otherwise, if such a line passes through $\mathbf{r}$, then it has nine intersections with the cusp curve. It follows, by Bezout's theorem, that the line is a component of the cusp curve, which is a contradiction.

Therefore, other than the four 4-fold points, any point $\mathbf{r}$ of the cusp curve is on a unique *proper* conic $C_{\mathbf{r}}$ that passes through the four 4-fold points, since a proper conic is uniquely determined by five points with no three of the five points being collinear. Since this proper (hence, also irreducible) conic $C_{\mathbf{r}}$ has $4 + 1 > 16$ intersections with the cusp curve, by Bezout's theorem, $C_{\mathbf{r}}$ is a component of the cusp curve. This shows that the cusp curve is the union of a collection of proper conics. Since the cusp curve is of degree 8, we conclude that it consists of four proper conics, which are necessarily circles since they all pass through the circular points. This completes the proof. □

The points $(\pm q, 0)$ play a special role, since they correspond to the given data. If $(X,Y) = (-q, 0)$ (respectively $(X,Y) = (q, 0)$), then the control points $\mathbf{b}_0$ (respectively $\mathbf{b}_2$) and $\mathbf{b}_1$ of the preimage curve are both mapped to $\mathbf{Q}_0$ (respectively $\mathbf{Q}_1$).

The four circles of this proposition will be called the *cusp circles*. After analyzing several examples we were led to formulate the following conjecture.

Conjecture 3. *Two of the four cusp circles are real, while the other two are conjugate-complex.*

Despite several efforts we were not able to prove (or disprove) this conjecture, as computer algebra tools which are available to us failed to find a symbolic factorization of the polynomial $c(X,Y)$.

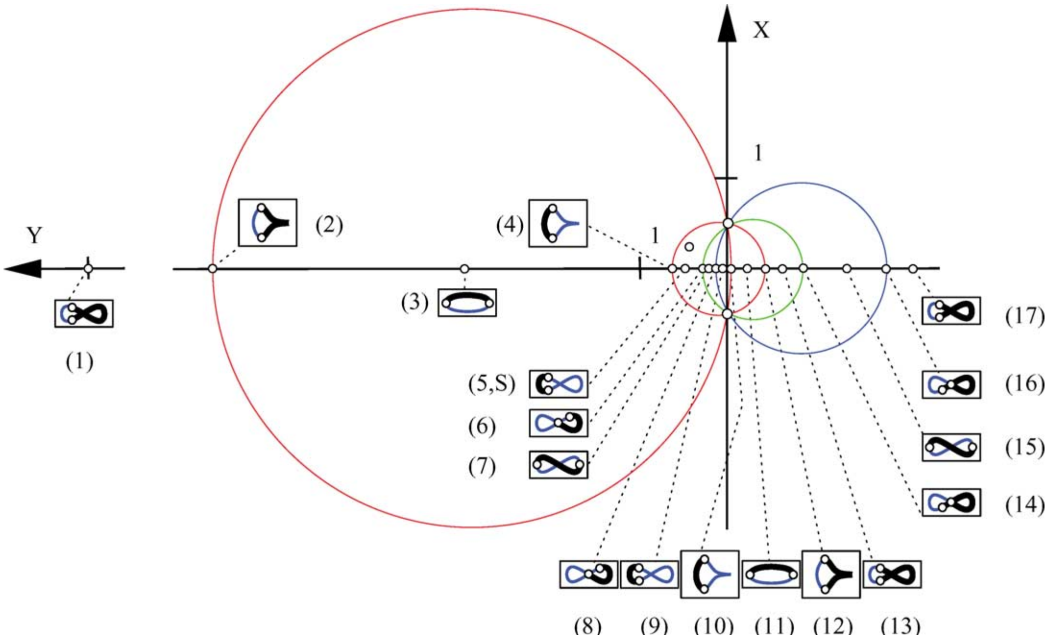

Fig. 3. Characterization diagram with cusp curve (red) and double point curves (green and blue). The points (1) ... (17) and (S) correspond to examples of interpolating curves, see Figs. 4 and 5.

They succeeded, however, in all examples, where we randomly chose rational numbers as input data S_1, S_2, T_1, T_2 and q. Apparently, the difficulties are caused by the fact that factoring the equation involves the symbolic solution of a univariate equation of degree 4.

An example is shown in Fig. 3 (cf. Section 5.4). The real part of the cusp curve leads to the red circles. Both circles are symmetric with respect to the Y-axis and intersect in the two points $(\pm q, 0)$.

5.3. Boundary double points

Assume that the quartic curve is not a circular arc. Then, the spherical quartic curve $\mathbf{x}(t)$ has a double point or a cusp at $t = 0$, if and only if there is a projecting line (3) intersecting $\mathbf{p}(0) = \mathbf{b}_0$ and another point $\mathbf{p}(t_0)$ of the preimage curve. Equivalently, the projecting line through $\mathbf{b}_0$ and the control points $\mathbf{b}_1$, $\mathbf{b}_2$ have to be coplanar. This leads to the following double point condition.

Theorem 4. *Assume that the Hermite data is non-circular. The spherical quartic curve has a double point at $t = 0$ (respectively at $t = 1$), if and only if*

$$\begin{aligned} d_0(X, Y) &= 2S_1q^3Y + 2S_1qY - S_2q^2 + S_2X^2 + S_2Y^2 = 0. \\ (\text{respectively } d_1(X, Y) &= -2T_1q^3Y - 2T_1qY - T_2q^2 + T_2X^2 + T_2Y^2 = 0). \end{aligned} \tag{22}$$

The polynomials $d_0(X, Y) = 0$ and $d_1(X, Y) = 0$ define two circles in the XY-plane. Both circles are symmetric with respect to the Y-axis and intersect in the two points $(\pm q, 0)$.

Proof. Non-circular data cannot be interpolated by a circular arc. Consequently, the preimage curve is not a straight line. Thus, if the projecting line through $\mathbf{b}_0$ is coplanar with $\mathbf{b}_1$ and $\mathbf{b}_2$, then it either intersects the curve in another point, leading to a double point, or it is tangent to it at $\mathbf{b}_0$, leading to a cusp.

The coplanarity is guaranteed by $d_0 = 0$, as this polynomial is the determinant of the matrix with rows $(1, -q, 0, 0)$, $(0, 0, q, 1)$, $\mathbf{b}_1$ and $\mathbf{b}_2$. The case $t = 1$ follows similarly.

The two conics $d_0(X, Y) = 0$ and $d_1(X, Y) = 0$ are circles, since they pass through the circular points at infinity. In addition, they can be shown to pass through the two points $(\pm q, 0)$. □

The two circles will be referred to as the *boundary double point circles*. Clearly, they intersect the cusp curve only in the two points $(\pm q, 0)$.

Along with the cusp curve, the double point circles can be used to define a characterization diagram, which governs the shape of the interpolating quartic curve. An example is shown in Fig. 3. The boundary point circles are shown in green and blue.

5.4. An example

We apply the theoretical results to the example

$$q = \frac{1}{2}, \qquad S_1 = -\frac{3}{2}, \qquad S_2 = -\frac{7}{2}, \qquad T_1 = -2, \qquad T_2 = \frac{3}{2}. \tag{23}$$

The double point circles (green and blue) and the cusp curve (red) are shown in Fig. 3. We have generated 18 different examples of interpolating curves. They are shown in Figs. 4 and 5.

The first examples $(1 \ldots 17)$ correspond to the intersections of the cusp curve and the double point circles with the Y-axis (even numbers), and to points in between them (odd numbers). The last example (S) has been constructed with the help of (non-generalized) stereographic projection, where the center has been fixed at the 'north pole' of the unit sphere. For all 18 examples, the corresponding (X, Y) points have been marked in Fig. 3.

In all examples, the curve segment obtained for $t \in [0, 1]$ is shown in black, and its end points are marked. The exterior part of the curve is represented by the two blue curve segments with the parameter domains $[-100, 0]$ and $[1, 101]$. In order to make the curve segments on the back side visible, the sphere is shown as a shaded 'stripe model'.

The type of each curve is represented by the "icon" on top of each plot: the black segment corresponds to $t \in [0, 1]$, and the blue curve represents the exterior part.

5.5. Characterization diagram

The cusp curve and the boundary double point circles define a *characterization diagram*, for spherical quartic curves, see Fig. 3. Each point in the diagram corresponds to a solution of the Hermite interpolation diagram, and vice versa. Within each cell of the diagram, the solutions have the same shape.

By crossing a red curve, one will "destroy" or "create" a double point. By crossing a blue or green curve, one of the two parameter values of a double point will cross one of the segment boundaries.

The different shapes are represented by the "icons" in Fig. 3. Again, the black segment corresponds to $t \in [0, 1]$, and the blue curve represents the exterior part. The boundaries are marked by two points. The limit shapes (curves with cusps or boundary double points) are associated with curves in the diagram (cusp curve or boundary point circles). The other shapes correspond to regions (bounded by the various

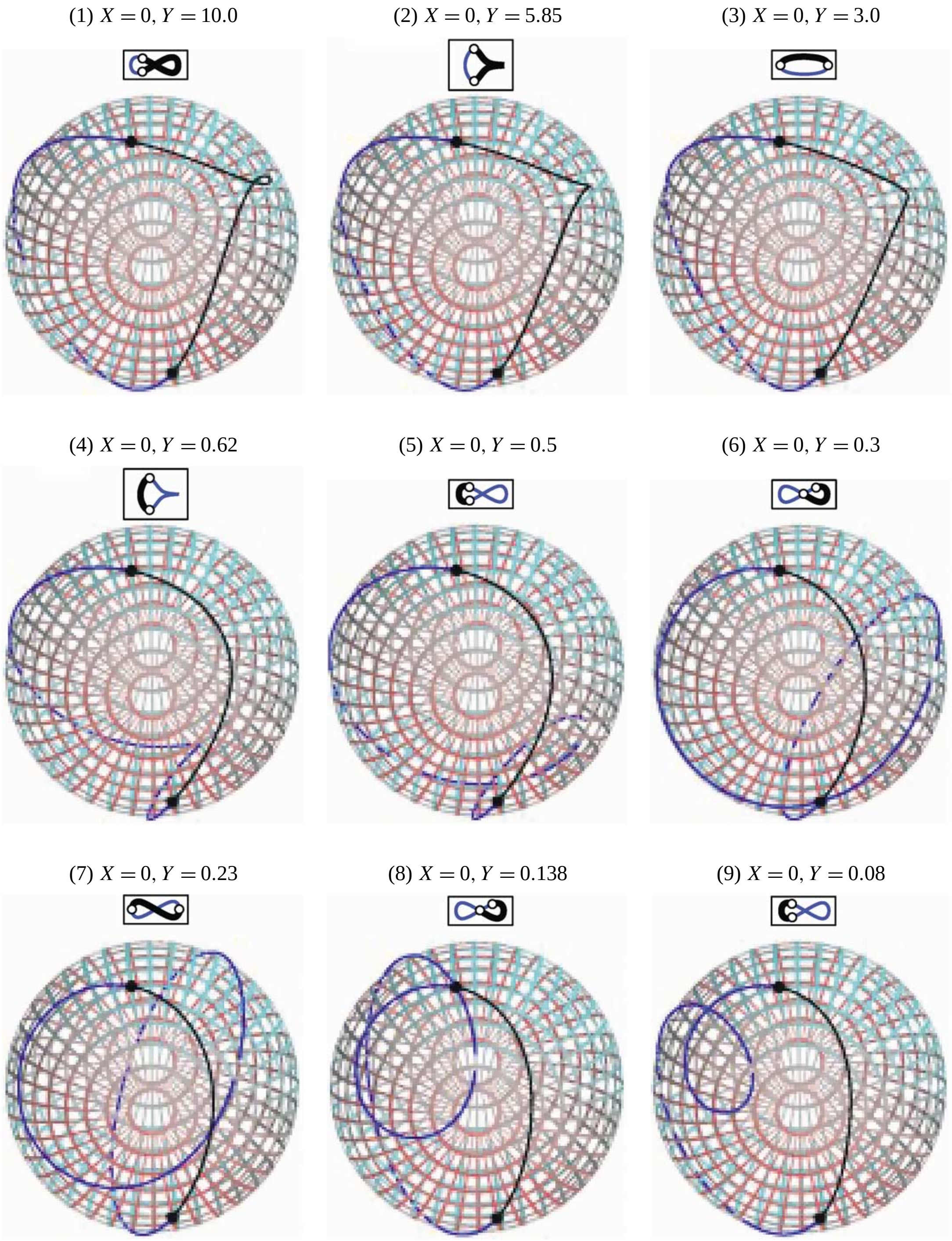

Fig. 4. Examples—interpolating curves with various shapes (1–9).

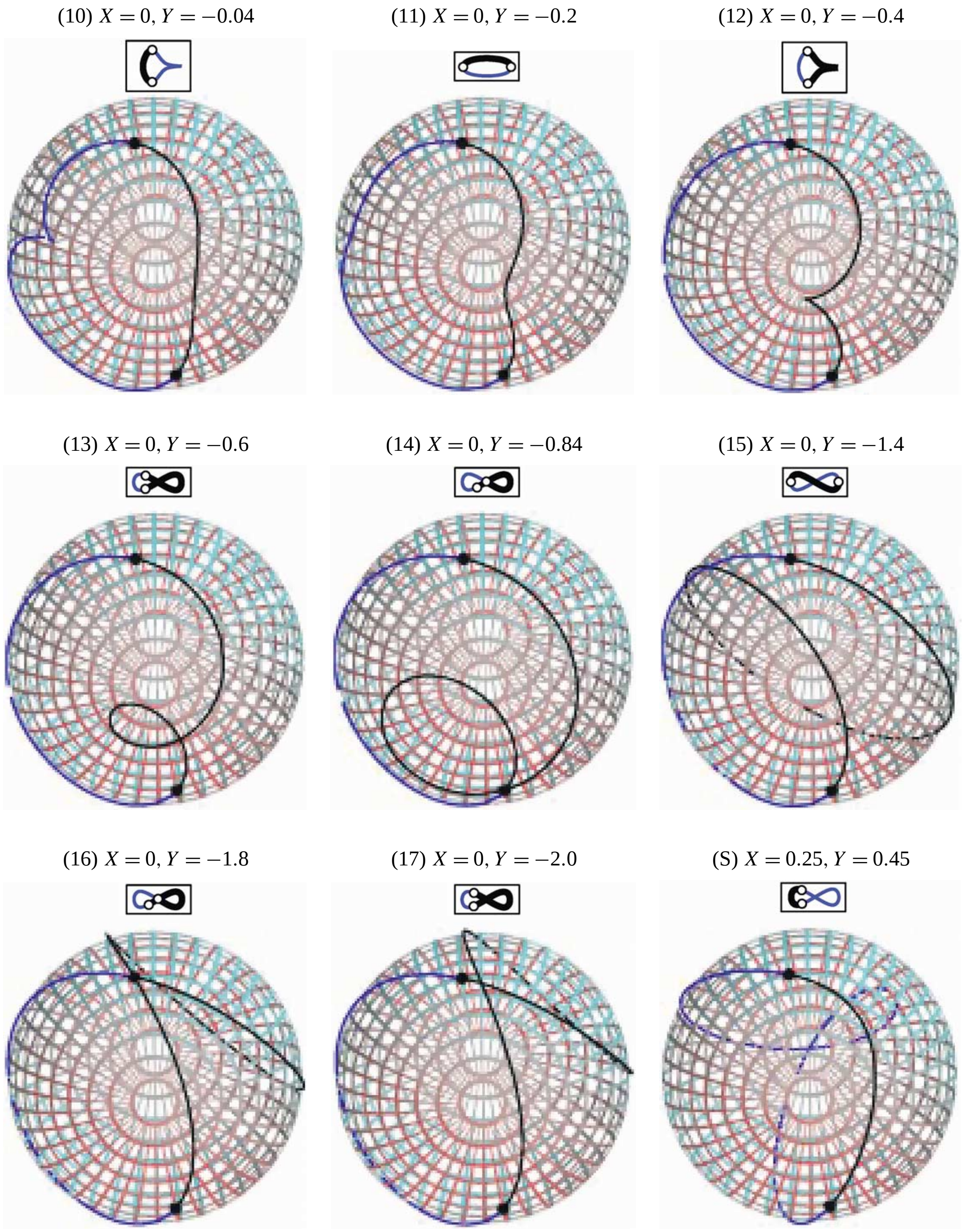

Fig. 5. Examples—interpolating curves with various shapes (10–17, S).

circles) of the diagram. There are 8 different shapes, corresponding to the cells and the boundaries of the characterization diagram.

Finally, it should be noted that the case of circular data (coplanar points and derivatives) requires a separate, more detailed analysis. Here, the double point circles and the cusp curve degenerate in various ways into circles with higher multiplicities, depending on whether the data admits a quadratic parameterization or not.

6. Concluding remarks

We discussed the problem of interpolating C^1 Hermite data on the sphere (two points with associated first derivative vectors) by rational spherical quartics. Using the generalized stereographic projection (Dietz et al., 1993), we obtained a two-parameter family of rational quartics which solve this problem. The shape of the solutions can be analyzed with the help of a characterization diagram, which describes the relation between the shape of the solutions and the two free parameters.

Our results can be used to develop a practical scheme for spherical Hermite interpolation, which would generate quartic spherical C^1 Hermite splines. Clearly, for each segment of the spline, the remaining two degrees of freedom have to be dealt with appropriately. This could be based on suitable heuristic techniques, or using numerical methods for minimizing a suitable fairness measure. Both approaches should take the shape of the solution into account.

We conclude this paper by pointing to two possible applications of quartic spherical C^1 Hermite splines. First, they can be useful for designing quintic spatial *Pythagorean hodograph curves*, since the hodograph of these curves corresponds to a spherical rational curve (see (Farouki et al., 2002)). Second, if they are used for generating *rational motions* (rigid body motions with rational point trajectories, see (Jüttler and Wagner, 2002)), they provide an interpolation scheme which has the property of "invariance with respect to parameterization", as it was called by Röschel (1998). So far, only the scheme of Gfrerrer (1999) provides this property.

Acknowledgements

The authors are extremely grateful to the referees for their comments which have helped to improve the manuscript. In particular, we are indebted to one of them for providing the proof of Proposition 2. Wenping Wang's work is supported by a grant (HKU 7032/99E) of Hong Kong Research Grant Council.

Appendix A

For the convenience of the reader, we provide a listing of the Maple code used for generating the criteria for cusps and double points.

```
> restart: with(linalg): with(plots):
> # preimage curve; boundary control points
> b0:=evalm(lambda0*[1,-q,0,0]+mu0*[0,0,q,1]);
```

```
> b2:=evalm(lambda1*[1,q,0,0]+mu1*[0,0,-q,1]);
> # components X and Y of b1 serve as free parameters
> b1:=[1,X,Y,0];
> # preimage curve; s=(1-t)
> p:=evalm(s^2*b0+2*s*t*b1+t^2*b2);
> # derivative
> pd:=evalm(2*(s*(b1-b0)+t*(b2-b1)));
> # generalized stereographic projection
> gsp:=proc(d)
> RETURN([ d[1]^2+d[2]^2+d[3]^2+d[4]^2,  2*d[1]*d[2]-2*d[3]*d[4],
>   2*d[2]*d[4]+2*d[1]*d[3],  d[2]^2+d[3]^2-d[1]^2-d[4]^2 ]);
> end;
> # image curve
> x:=subs(s=(1-t), gsp(p)):
> # control points of image curve
> for i from 0 to 4 do
> map(factor,evalm(map(coeff,map(coeff,gsp(p),s,i),t,4-i)
  /binomial(4,i)));
> od:
> # image curve in Cartesian coordinates
> xc:=[x[2]/x[1],x[3]/x[1],x[4]/x[1]]:
> # derivative
> xcd:=map(diff,xc,t):
> # derivatives at segment boundaries
> xcd0:=map(factor,subs(t=0,eval(xcd)));
> xcd1:=map(factor,subs(t=1,eval(xcd)));
> # C1 boundary conditions: interpolation of 1st derivatives
> res0:=subs(lambda0=lambda0s,mu0=mu0s,solve({xcd0[1]=T1*(q^2-1)
             /(1+q^2), xcd0[2]=T2/(1+q^2)}, {lambda0,mu0}));
> res1:=subs(lambda1=lambda1s,mu1=mu1s,solve({xcd1[1]=S1*(q^2-1)
             /(q^2+1), xcd1[2]=S2/(q^2+1)}, {lambda1, mu1}));
> assign(res0); assign(res1);
> ressubs:= lambda0=lambda0s, mu0=mu0s, lambda1=lambda1s, mu1=mu1s:
> # substitute results into preimage control points
> b0s:=subs(ressubs,eval(b0)): b2s:=subs(ressubs,eval(b2)):
> auxfac:=(T1^2+q^4*T1^2+T2^2+2*q^2*T1^2)
         *(S1^2+2*q^2*S1^2+q^4*S1^2+S2^2);
> # substitute results into preimage curve
> pint:=map(factor,subs(ressubs, s=(1-t),eval(p))):
> # its derivative points
> pintd:=map(factor,subs(ressubs, s=(1-t),eval(pd))):
> # cusp condition
> g01:=factor(auxfac*(pint[1]*pintd[2]-pint[2]*pintd[1])):
> g02:=factor(auxfac*(pint[1]*pintd[3]-pint[3]*pintd[1])):
> g23:=factor(auxfac*(pint[3]*pintd[4]-pint[4]*pintd[3])):
> g31:=factor(auxfac*(pint[4]*pintd[2]-pint[2]*pintd[4])):
> cc:=factor(resultant(g01-g23,g02-g31, t)/(8192*auxfac^2)):
> factor(subs(Y=0,cc));
> # condition for a double point at t=0
> db0:=numer(factor(1/q/8*det(subs(ressubs,matrix(4,4,[1,-q,0,0,0,0,
          q,1,1,X,Y,0,b2[1],b2[2],b2[3],b2[4]])))));
> # condition for a double point at t=1
> db1:=numer(factor(1/q/8*det(subs(ressubs, mu1=mu1s,matrix(4,4,[1,q,
          0,0,0,0,-q,1,1,X,Y,0,b0[1],b0[2],b0[3],b0[4]])))));
```

References

Choi, H.I., Lee, D.S., Moon, H.P., 2002. Clifford algebra, spin representation, and rational parameterization of curves and surfaces. Adv. Comput. Math. 17, 5–48.

Dickson, L.E., 1952. History of the Theory of Numbers, Vol. II. Chelsea, New York.
Dietz, R., Hoschek, J., Jüttler, B., 1993. An algebraic approach to curves and surfaces on the sphere and on other quadrics. Computer Aided Geometry Design 10, 211–229.
Farouki, R.T., 2002. Pythagorean-hodograph curves. In: Farin, G., Hoschek, J., Kim, M.-S. (Eds.), Handbook of Computer Aided Geometric Design. Elsevier, Amsterdam, pp. 405–428.
Farouki, R.T., al-Kandari, M., Sakkalis, T., 2002. Hermite interpolation by rotation-invariant spatial Pythagorean-hodograph curves. Adv. Comput. Math. 17, 369–383.
Gfrerrer, A., 1999. Rational interpolation on a hypersphere. Computer Aided Geometric Design 16, 21–37.
Hoschek, J., Seemann, G., 1992. Spherical splines. RAIRO Modél. Math. Anal. Numér. 26, 1–22.
Jupp, P.E., Kent, J.T., 1987. Fitting smooth paths to spherical data. J. Roy. Stat. Soc. Ser. C 36, 34–46.
Jüttler, B., Wagner, M.G., 2002. Kinematics and animation. In: Farin, G., Hoschek, J., Kim, M.-S. (Eds.), Handbook of Computer Aided Geometric Design. Elsevier, Amsterdam, pp. 723–748.
Kim, M.-S., Nam, K.-W., 1995. Interpolating solid orientations with circular blending quaternion curves. Computer-Aided Design 27, 385–398.
Kim, M.-J., Kim, M.-S., Shin, S., 1995. A general construction scheme for unit quaternion curves with simple high order derivatives. Computer Graphics (SIGGRAPH) 29, 369–376.
Nielson, G.M., Heiland, R.W., 1992. Animated rotations using quaternions and splines on a 4D sphere. Program. Comput. Softw. 18, 145–154.
Noakes, L., 1998. Non-linear corner cutting. Adv. Comput. Math. 8, 165–177.
Pletinckx, D., 1989. Quaternion calculus as a basic tool in computer graphics. The Visual Comput. 5, 2–13.
Shoemake, K., 1985. Animating rotations with quaternion curves. Computer Graphics (SIGGRAPH) 19, 245–254.
Pottmann, H., Wallner, J., 2001. Computational Line Geometry. Springer, Berlin.
Röschel, O., 1998. Rational motion design—a survey. Computer-Aided Design 30, 169–178.
Wang, W., Joe, B., 1993. Orientation interpolation in quaternion space using spherical biarcs. In: Proceedings of Graphics Interface ’93, pp. 24–32.
Wang, W., Joe, B., 1997. Interpolation on quadric surfaces with rational quadratic spline curves. Computer Aided Geometric Design 14, 207–230.
Wang, W., Qin, K., 2000. Existence and computation of spherical rational quartic curves for Hermite interpolation. The Visual Comput. 16, 187–196.